J|A|C|S
ARTICLES
Published on Web 03/21/2006

Internal Water Molecules and Magnetic Relaxation in Agarose Gels

Fabian Vaca Chávez,† Erik Persson, and Bertil Halle*

Contribution from the Department of Biophysical Chemistry, Lund University, SE-22100 Lund, Sweden

Received January 6, 2006; E-mail: bertil.halle@bpc.lu.se

Abstract: Agarose gels have long been known to produce exceptionally large enhancements of the water ^{1}H and ^{2}H magnetic relaxation rates. The molecular basis for this effect has not been clearly established, despite its potential importance for a wide range of applications of agarose gels, including their use as biological tissue models in magnetic resonance imaging. To resolve this issue, we have measured the ^{2}H magnetic relaxation dispersion profile from agarose gels over more than 4 frequency decades. We find a very large dispersion, which, at neutral pH, is produced entirely by internal water molecules, exchanging with bulk water on the time scale 10^{-8}−10^{-6} s. The most long-lived of these dominate the dispersion and give rise to a temperature maximum in the low-frequency relaxation rate. At acidic pH, there is also a low-frequency contribution from hydroxyl deuterons exchanging on a time scale of 10^{-4} s. Our analysis of the dispersion profiles is based on a nonperturbative relaxation theory that remains valid outside the conventional motional-narrowing regime. The results of this analysis suggest that the internal water molecules responsible for the dispersion are located in the central cavity of the agarose double helix, as previously proposed on the basis of fiber diffraction data. The magnetic relaxation mechanism invoked here, where spin relaxation is induced directly by molecular exchange, also provides a molecular basis for understanding the water ^{1}H relaxation behavior that governs the intrinsic magnetic resonance image contrast in biological tissue.

1. Introduction

Agarose is a linear polysaccharide derived from the cell wall of agar-bearing marine red algae of the *Rhodophyceae* family.[1] The principal disaccharide repeating unit of agarose, called agarobiose, is composed of 1,3-linked β-D-galactopyranose and 1,4-linked 3,6-anhydro-α-L-galactopyranose residues (Figure 1a),[2] henceforth denoted by GAL and AGL, respectively. In aqueous solution, agarose behaves as a semiflexible polymer at high temperatures, but below ∼35 °C it adopts an ordered double-helical conformation. Subsequent lateral aggregation leads to fibrils containing six or more double helices, which, at concentrations above ∼0.1%, form a percolating three-dimensional gel network with a high elastic modulus.[3−7] The microstructure of agarose gels has not been firmly established, but X-ray diffraction patterns from films made by drying and stretching agarose gels at low temperatures are consistent with a double-helical structure.[8] The agarose double helix is built from two parallel, left-handed helices with three agarobiose units per turn.[8] It has been proposed that this structure is stabilized by a string of internal water molecules in the narrow channel that extends along the helix axis (Figure 1b).[8]

Molecular-level information about the structure and dynamics of native gels is contained in the magnetic relaxation rates associated with the water NMR signal. It has long been known that gelation of agarose is accompanied by a dramatic broadening of the water ^{1}H resonance; the transverse relaxation rate, R_2, increasing by 2 orders of magnitude even at agarose concentrations of a few percent.[9−11] In contrast, little or no relaxation enhancement was observed upon gelation of starch, cellulose derivatives, or gelatin. The exceptional relaxation enhancement in agarose gels was originally attributed to a long-ranged perturbation of the bulk water in the gel, induced by a peculiar matching of the agarose molecule to the presumed "icelike" water structure.[9,10] Similar ideas of surface-induced long-range ordering and slowing down of water were invoked to explain water ^{1}H and ^{2}H relaxation enhancements in other gels and in biological tissues.[12−14] If these ideas were correct,

† Present address: Institut für Physikalische Chemie, Universität Münster, DE-48149 Münster, Germany.

(1) Murano, E. *J. Appl. Phycol.* **1995**, *7*, 245−254.
(2) Lahaye, M.; Rochas, C. *Hydrobiologia* **1991**, *221*, 137−148.
(3) Djabourov, M.; Clark, A. H.; Rowlands, D. W.; Ross-Murphy, S. B. *Macromolecules* **1989**, *22*, 180−188.
(4) Whytock, S.; Finch, J. *Biopolymers* **1991**, *31*, 1025−1028.
(5) Sugiyama, J.; Rochas, C.; Turquois, T.; Taravel, F.; Chanzy, H. *Carbohydr. Polym.* **1994**, *23*, 261−264.
(6) Normand, V.; Lootens, D. L.; Amici, E.; Plucknett, K. P.; Aymard, P. *Biomacromolecules* **2000**, *1*, 730−738.
(7) Aymard, P.; Martin, D. R.; Plucknett, K. P.; Foster, T. J.; Clark, A. H.; Norton, I. T. *Biopolymers* **2001**, *59*, 131−144.
(8) Arnott, S.; Fulmer, A.; Scott, W. E.; Dea, I. C. M.; Moorhouse, R.; Rees, D. A. *J. Mol. Biol.* **1974**, *90*, 269−284.
(9) Hechter, O.; Wittstruck, T.; McNiven, N.; Lester, G. *Proc. Natl. Acad. Sci. U.S.A.* **1960**, *46*, 783−787.
(10) Sterling, C.; Masuzawa, M. *Makromol. Chem.* **1968**, *116*, 140−145.
(11) Child, T. F.; Pryce, N. G.; Tait, M. J.; Ablett, S. *Chem. Commun.* **1970**, 1214−1215.
(12) Collison, R.; McDonald, M. P. *Nature* **1960**, *186*, 548−549.
(13) Hazlewood, C. F.; Nichols, B. L.; Chamberlain, N. F. *Nature* **1969**, *222*, 747−750.

10.1021/ja058837n CCC: $33.50

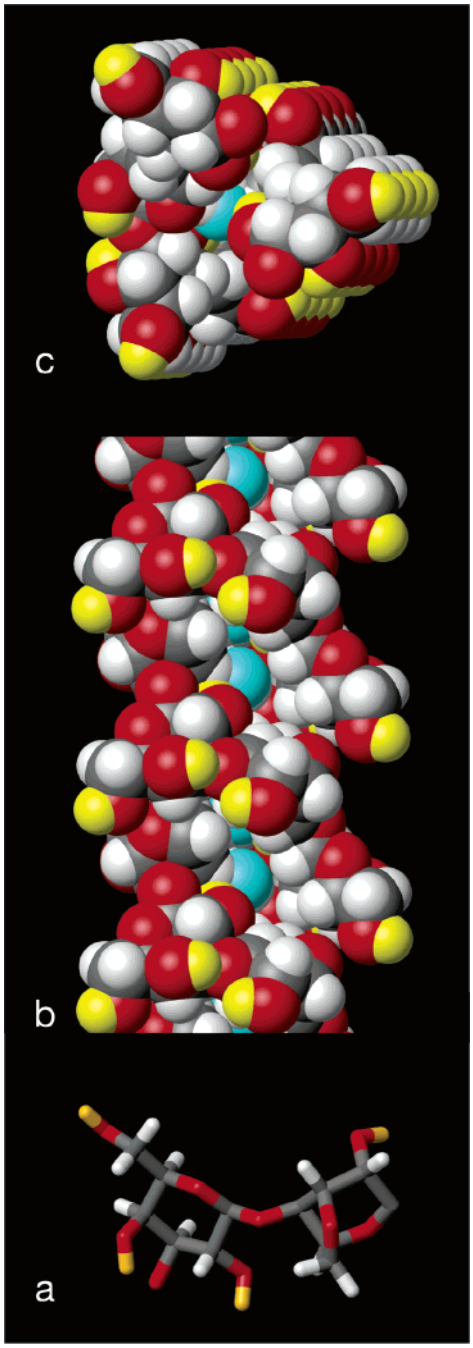

Figure 1. Agarose structure based on atomic coordinates from fiber X-ray crystallography[8] (PDB file 1AGA) with hydrogen atoms and internal water molecules added (see text): (a) agarobiose unit; (b) side view of double helix; (c) tilted top view of double helix. Hydroxyl hydrogens (yellow) and internal water molecules (cyan) are highlighted.

one would also expect a large reduction of the water self-diffusion coefficient, D, in these systems. This is not observed.[15−17] For example, in a 7% agar gel, with a 400-fold transverse relaxation enhancement,[9] D is reduced by merely 13% (and this is largely a trivial obstruction effect).[16] It was thus concluded that nearly all water molecules in the gel are unaffected by the agarose and that the transverse relaxation enhancement must come from a very small fraction of bound water molecules or from exchanging hydroxyl protons.[16] Subsequent measurements of the longitudinal (R_1), transverse (R_2), and rotating-frame ($R_{1\rho}$) water ^{1}H and ^{2}H relaxation rates in agarose (or agar) gels as a function of temperature, agarose concentration, and water H/D isotope fraction indicated that molecular motions on at least two time scales (nanoseconds and microseconds) are involved.[18−20] However, for reasons that will become clear in the following, these studies could not fully elucidate the molecular origins of the observed relaxation effects.

The aim of the present study is to identify and to characterize quantitatively the molecular species and motions responsible for the relaxation enhancement in agarose gels. We focus on ^{2}H relaxation, which is easier to analyze than ^{1}H data because it is governed by the single-spin quadrupole mechanism.[21] The interpretation of relaxation data from complex systems with motions on several time scales becomes highly model-dependent unless the data extend over a wide range of NMR frequencies (or magnetic fields). Whereas previous studies of agarose gels have been restricted to relatively high frequencies (>2 MHz), we report ^{2}H magnetic relaxation dispersion (MRD) profiles extending down to 1.5 kHz and covering more than 4 frequency decades.

Another decisive element of our approach concerns the theoretical foundations of nuclear spin relaxation. In all previous water NMR relaxation studies of gels, the interpretation was based on the conventional second-order perturbation theory of spin relaxation, also known as the Bloch−Wangsness−Redfield (BWR) theory.[21,22] This theory is valid in the so-called motional narrowing regime, where the rate of thermal (stochastic) modulation of the relevant nuclear coupling is higher than the frequency of coherent spin evolution that would be induced by that coupling in the absence of fluctuations. For ^{2}H relaxation, this means that all motional correlation times must be shorter than $\sim$1 μs. However, in the agarose gels investigated here, the dominant relaxation dispersion is associated with molecular motions on the time scale 1−100 μs, well outside the range of validity of BWR theory. We therefore employ a more general, nonperturbative relaxation theory, based on an analytical solution of the appropriate stochastic Liouville equation (SLE).[23]

Agarose gels have been widely used to model the ^{1}H magnetic relaxation behavior of biological tissues, which largely determines the intrinsic contrast in magnetic resonance imaging (MRI).[24−26] In this connection, water ^{1}H MRD profiles from agarose gels have been reported, but a molecular interpretation was not given.[24,25] As reported elsewhere,[27] we have also recorded ^{1}H MRD profiles from 10 kHz to 200 MHz for agarose gel samples matching the ones investigated here by ^{2}H MRD. Mainly because of cross-relaxation among dipole-coupled

(14) Cope, F. W. *Biophys. J.* **1969**, *9*, 303−319.
(15) Nakayama, F. S.; Jackson, R. D. *J. Phys. Chem.* **1963**, *67*, 932−933.
(16) Woessner, D. E.; Snowden, B. S.; Chiu, Y.-C. *J. Colloid Interface Sci.* **1970**, *34*, 283−289.
(17) Derbyshire, W.; Duff, I. D. *Faraday Discuss. Chem. Soc.* **1974**, *57*, 243−254.
(18) Woessner, D. E.; Snowden, B. S. *J. Colloid Interface Sci.* **1970**, *34*, 290−299.
(19) Outhred, R. K.; George, E. P. *Biophys. J.* **1973**, *13*, 83−96.
(20) Andrasko, J. *Biophys. J.* **1975**, *15*, 1235−1243.
(21) Abragam, A. *The Principles of Nuclear Magnetism*; Clarendon Press: Oxford, 1961.
(22) Goldman, M. *J. Magn. Reson.* **2001**, *149*, 160−187.
(23) Halle, B. *Prog. NMR Spectrosc.* **1996**, *28*, 137−159.
(24) Walker, P. M.; Balmer, C.; Ablett, S.; Lerski, R. A. *Phys. Med. Biol.* **1989**, *34*, 5−22.
(25) Mendelson, D. A.; Heinsbergen, J. F.; Kennedy, S. D.; Szczepaniak, L. S.; Lester, C. C.; Bryant, R. G. *Magn. Reson. Imaging* **1991**, *9*, 975−978.
(26) Litt, H. I.; Brody, A. S. *Acad. Radiol.* **2001**, *8*, 377−383.
(27) Vaca Chávez, F.; Halle, B. *Magn. Reson. Med.*, in press.

protons, the interpretation of ^{1}H MRD data is more challenging.[28] The present ^{2}H MRD analysis simplifies this task by providing more direct access to some of the molecular parameters that determine the ^{1}H MRD profile. The motivation for the present study is thus two-fold: (*i*) to shed new light on the microstructure, dynamics, and hydration of agarose gels and (*ii*) to provide a quantitative basis for the interpretation of water relaxation data from aqueous gels and other systems that, like soft biological tissues, contain immobilized macromolecules in a mobile aqueous phase.

2. Materials and Methods

2.1. Gel Preparation. Agarose of an ultrapure grade marketed under the name Supra Sieve CPG was purchased from American Bioanalytical (Natick, MA) and was used as supplied. A small amount of residual sulfate groups may be present in agarose in the AGL.C2, GAL.C4, or GAL.C6 positions (with the usual labeling convention).[2] According to the manufacturer, this preparation has low (<0.12% w/w) sulfate content and low (<0.1) electroendosmosis (an electrophoretic flow effect caused by positive counterions). The gel setting temperature is specified as <35 °C, and the gel melting temperature, as <65 °C, both at 4% agarose. Another preparation, agarose CPG/LE, of higher gel strength and higher gel melting temperature (87 °C at 1.5% agarose) was also investigated, but no significant difference in the ^{2}H MRD profile was seen. Because of its higher melting temperature, the CPG/LE preparation was used to measure the temperature dependence of R_1 in the range 5−70 °C. The specifications of the CPG/LE preparation are identical to Sigma's agarose Type I-A, which has a weight-average molar mass, $\langle M_w \rangle = 170$ kg mol^{-1}, corresponding to 555 agarobiose units per chain, and a polydispersity index, $\langle M_w \rangle / \langle M_n \rangle = 1.7$.[7]

The gels were prepared directly in 10 mm o.d. NMR tubes by dissolving agarose in D_2O (99.9 atom % ^{2}H, low paramagnetic content) from Cambridge Isotope Laboratories (Andover, MA). The samples were immersed in a water bath at 99 °C for 30−40 min and were then cooled to 45 °C, where pH* was measured. The operational pH* (not corrected for H/D isotope effects) was 3.30 and 6.95 in the two MRD samples examined at 20 °C and 7.10 in the sample used for the variable-temperature experiment. These pH* values were obtained after microliter additions of HCl and NaOH, respectively. After pH* measurement, the samples were slowly (∼2 h) cooled to room temperature and were then kept at 16 °C for 1−2 days before MRD measurements. The total number, N_T, of water molecules per average monosaccharide of molar mass 153.2 g mol^{-1} was calculated under the assumption that the agarose preparation contains 5% w/w H_2O, as specified by the manufacturer. For the acidic and neutral samples, $N_T = 136.7$ and 123.0, respectively. To allow direct comparison of the results from these two samples, the relaxation data were normalized to $N_T = 130$, assuming that $R_1 - R_1^{(0)}$ is inversely proportional to N_T (see below). Here, $R_1^{(0)} = 2.64$ s^{-1} is the longitudinal ^{2}H relaxation rate measured at 20 °C on a reference sample of pure D_2O. The sample used for the variable-temperature study had $N_T = 124.6$.

2.2. MRD Experiments. The longitudinal relaxation rate, R_1, of the water ^{2}H magnetization was measured over more than 4 frequency decades, from 1.5 kHz to 30.7 MHz. To cover this frequency range, we used three types of NMR spectrometer: (1) a Stelar Spinmaster fast field-cycling (FC) spectrometer (1.5 kHz−1.5 MHz); (2) a field-variable iron-core magnet equipped with a Tecmag console (2.2−11.1 MHz); and (3) Bruker Avance DMX 100 and 200 spectrometers with conventional cryomagnets (15.4 and 30.7 MHz). The temperature was maintained at 20.0 ± 0.1 °C using a Stelar variable temperature control unit or a Bruker Eurotherm regulator (at the two highest frequencies). Temperatures were checked with a thermocouple referenced to an ice−water bath.

The FC technique overcomes the sensitivity problem of conventional fixed-field experiments in weak magnetic fields.[29,30] The prepolarized sequence (PP/S) was used with polarization and detection at 3.07 and 2.70 MHz, respectively. In the non-FC experiments (with variable detection field), R_1 was measured with the $180° - \tau - 90°$ inversion recovery sequence. Single-exponential recovery curves were obtained throughout, from which R_1 was determined by a three-parameter fit.

2.3. Analysis of MRD Data. Under the conditions of the present study, the relaxation of the longitudinal ^{2}H magnetization is caused entirely by thermal fluctuations of the nuclear quadrupole−electric field gradient interaction of water deuterons and agarose hydroxyl deuterons.[21] For both species, the field gradient tensor is very nearly axially symmetric, with the principal component along the O−D bond. The interaction strength is measured by the rigid-lattice quadrupole coupling constant, $\chi = 226$ kHz and 212 kHz for deuterons in (internal) D_2O molecules and in agarose OD groups, respectively.[31,32] Relaxation is induced by molecular motions that randomize the orientation of the O−D bond. Subpicosecond librations and fast hydroxyl group rotations do not contribute directly to the observed relaxation dispersion but scale the quadrupole interaction so that the slower motions modulate a residual quadrupole coupling, $S\chi$, where S is the rank-2 orientational order parameter of the O−D bond.[31]

An agarose gel is a microheterogeneous system, where water molecules in different local environments have different rotational correlation times. Operationally, we can distinguish water molecules with subnanosecond correlation times from those with longer correlation times. The former are in the so-called extreme-narrowing regime at all investigated frequencies and do not contribute to the observed relaxation dispersion. This category includes bulk water molecules that are not significantly affected by the agarose and water molecules in contact with the agarose surface. The latter are expected to be slowed in their rotational motion by a factor of 2 or less.[33−35] The water molecules that contribute to the relaxation dispersion have correlation times in the nanosecond to microsecond range. Except for the fast librations that establish the order parameter S, such water molecules can be considered irrotationally bound. The orientational randomization of the field gradient tensor (along the O−D bond) of these water molecules occurs by exchange with rapidly rotating bulk water. For these internal water molecules, trapped within the agarose fibrils in the gel, the correlation time can therefore be identified with the mean residence time at internal hydration sites.

In solutions of freely tumbling macromolecules, the relaxation dispersion can be described by conventional BWR theory as long as the correlation time of internal water molecules (i.e., the macromolecular tumbling time) is shorter than ∼1 μs, but without any restrictions on the rate of exchange between internal and bulk water.[23] In contrast, when relaxation is induced by the exchange process itself, as in a gel with immobilized macromolecules, the BWR theory is only valid in the fast-exchange regime. This situation has been treated by a more general SLE approach, which shows that the usual fast-exchange BWR expressions remain valid to an excellent approximation for all values of the correlation (residence) time, provided that only a small fraction of the water molecules are irrotationally bound (the so-called dilute regime).[23,28,36,37] However, the Larmor frequency must then be replaced by an effective frequency (see below). The agarose hydroxyl deuterons, which have even longer residence times than the internal water molecules, can be treated in the same way.

(28) Halle, B. *Magn. Reson. Med.*, in press.
(29) Noack, F. *Prog. NMR Spectrosc.* **1986**, *18*, 171−276.
(30) Ferrante, G.; Sykora, S. *Adv. Inorg. Chem.* **2005**, *57*, 405−470.
(31) Halle, B.; Denisov, V. P.; Venu, K. In *Biological Magnetic Resonance*; Krishna, N. R., Berliner, L. J., Eds.; Kluwer/Plenum: New York, 1999; pp 419−484.
(32) Denisov, V. P.; Halle, B. *J. Mol. Biol.* **1995**, *245*, 698−709.
(33) Uedaira, H.; Ikura, M.; Uedaira, H. *Bull. Chem. Soc. Jpn.* **1989**, *62*, 1−4.
(34) Thomas, T. O.; Leyte, J. C. *Mol. Phys.* **1997**, *91*, 715−723.
(35) Halle, B. *Philos. Trans. R. Soc. London, Series B* **2004**, *359*, 1207−1224.
(36) Halle, B.; Denisov, V. P. *Biophys. J.* **1995**, *69*, 242−249.
(37) Roose, P.; Bauwin, H.; Halle, B. *J. Phys. Chem. B* **1999**, *103*, 5167−5174.

From the preceding considerations, it follows that the observed longitudinal ^{2}H relaxation rate can be expressed as

$$R_1(\omega_0) = \left(1 - \sum_k f_k\right) R_1^{(0)} + \sum_k f_k R_1^{(k)}(\omega_0) \quad (1)$$

where $\omega_0 = 2\pi\nu_0$ is the angular Larmor frequency and f_k is the fraction of deuterons in environment k:

$$f_k = \frac{n_k}{\sum_k n_k} = \frac{N_k}{N_T} \quad (2)$$

Here, N_k is the number of water molecules (or pairs of hydroxyl groups) of type k per average monosaccharide, and N_T is the total number of water molecules per monosaccharide. With 4 hydroxyl groups per agarobiose unit (Figure 1a), $N_{OD} = 1$ if all hydroxyl groups are solvent-exposed and less if some of them are inaccessible (as in a fibril). Since $N_T = 130 \gg N_{OD}$, we can neglect the hydroxyl contribution to N_T. The intrinsic relaxation rate in environment k is given by[23]

$$R_1^{(k)}(\omega_0) = \frac{2}{3}\Omega_{Q,k}^2[0.2\tilde{J}^{(k)}(\omega_0) + 0.8\tilde{J}^{(k)}(2\omega_0)] \quad (3)$$

Here we have introduced the generalized spectral density function

$$\tilde{J}^{(k)}(m\omega_0) = \frac{\tau_k}{1 + (\omega_{k,m}^{\text{eff}}\tau_k)^2} \quad (4)$$

and the effective frequency

$$\omega_{k,m}^{\text{eff}} = [\Omega_{Q,k}^2 + (m\omega_0)^2]^{1/2} \quad (5)$$

The residual quadrupole frequency appearing in eqs 3 and 5 is defined as

$$\Omega_{Q,k} = \frac{3\pi}{2} S_k \chi_k \quad (6)$$

In the motional narrowing regime, which for longitudinal relaxation is defined by the inequality $(\Omega_{Q,k}\tau_k)^2 \ll 1 + (\omega_0\tau_k)^2$, the generalized spectral density in eq 4 reduces to the usual spectral density, $J^{(k)}(m\omega_0) = \tau_k/[1 + (m\omega_0\tau_k)^2]$.

In the limit $(\omega_{k,m}^{\text{eff}}\tau_k)^2 \gg 1$, which applies to the hydroxyl deuterons at all Larmor frequencies ω_0, eqs 3−5 yield

$$R_1^{(k)}(\omega_0) = \frac{2}{3\tau_k}\left[\frac{0.2}{1 + (\omega_0/\Omega_{Q,k})^2} + \frac{0.8}{1 + (2\omega_0/\Omega_{Q,k})^2}\right] \quad (7)$$

In this limit, the dispersion profile still has a Lorentzian shape, but the dispersion frequency is the quadrupole frequency $\Omega_{Q,k}$ rather than the inverse correlation time. Thus, in this adiabatic regime, molecular motions have no effect on the position (on the frequency axis) of the dispersion but only scale its amplitude. The integral of the dispersion profile is $(\pi/5)\Omega_{Q,k}/\tau_k$, a factor $\Omega_{Q,k}\tau_k \gg 1$ smaller than in the motional-narrowing regime. We note that eq 7 is essentially identical to an expression for dipolar ^{1}H relaxation by infrequent jumps, derived with the aid of a spin temperature approximation.[38] Our expression differs in the numerical factors and in the appearance of a "double-quantum" term, both resulting from the fact that a spin-1 nucleus is a three-level system.

(38) Slichter, C. P.; Ailion, D. *Phys. Rev.* **1964**, *135*, A1099-A1110.

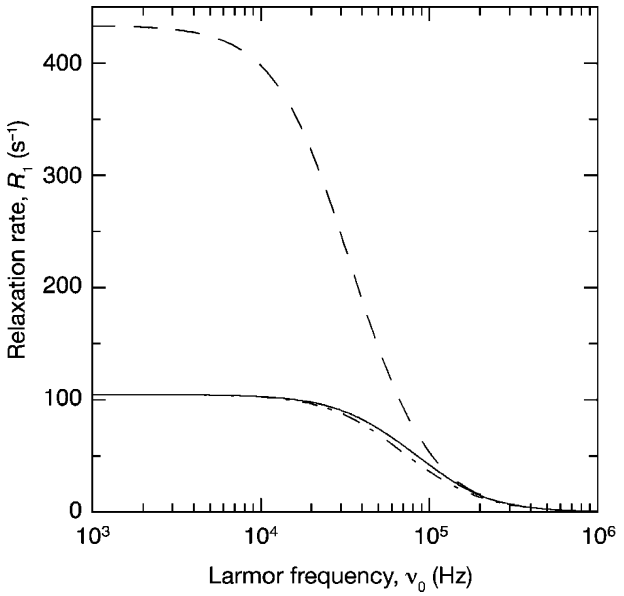

Figure 2. Contribution to the ^{2}H dispersion from the most long-lived internal water molecules (component W3) calculated with parameter values from the fit in Figure 3 and using the exact SLE expression (solid curve), the approximate SLE expression, eqs 3−5 (dash−dotted curve), or the conventional motional-narrowing theory (dashed curve).

Fits to the dispersion profiles were made with the Levenberg−Marquardt nonlinear least-squares algorithm[39] with equal weighting of all data points. Quoted uncertainties in parameter values (one standard deviation) are based on an estimated 1% accuracy in all R_1 values and were obtained with the Monte Carlo method[39] using 1000 synthetic data sets. The target function for the fit was eq 1, written in the form

$$R_1(\omega_0) = \alpha + f_{W1}R_1^{W1}(\omega_0) + f_{W2}R_1^{W2}(\omega_0) + f_{W3}R_1^{W3}(\omega_0) + f_{OD}R_1^{OD}(\omega_0) \quad (8)$$

The first term includes all frequency-independent contributions to R_1, notably from the bulk water phase and from the mobile hydration layer at the surface of the agarose fibrils. An adequate description of the data requires three water correlation times. Two of these (denoted W1 and W2) are in the motional-narrowing regime and are therefore described by two parameters each: $N_{W1}S_{W1}^2$ and τ_{W1}, and similarly for component W2. The third water component (W3) is outside the motional-narrowing regime and must therefore be described with the generalized spectral density function in eq 4. For the fit, we actually used the exact result for the dilute regime, a lengthy analytical expression that reduces to eqs 3−5 when higher-order cross-terms in $\omega_0\tau_k$ and $\Omega_{Q,k}\tau_k$ are neglected (B. Halle and T. Nilsson, to be published). Although the exact result differs little in its numerical predictions from the approximate expression (Figure 2), it is preferred because it allows us to determine the parameters N_{W3} and S_{W3} individually. The last term in eq 8 represents the contribution from hydroxyl deuterons, which was modeled by eq 7. This contribution is described by two parameters: x_{OD}/τ_{OD} and S_{OD}, where x_{OD} is the fraction accessible (exchanging) hydroxyl groups in the agarose fibrils.

3. Results and Discussion

3.1. ^{2}H MRD Profiles at Neutral and Acidic pH. Figure 3 shows the water ^{2}H R_1 dispersions obtained at 20.0 °C from identically prepared agarose/D_2O gels at two pD values. The effect of the slight concentration difference between the two

(39) Press: W. H.; Teukolsky, S. A.; Vetterling, W. T.; Flannery, B. P. *Numerical Recipes in C*, 2nd ed.; Cambridge University Press: Cambridge, 1992.

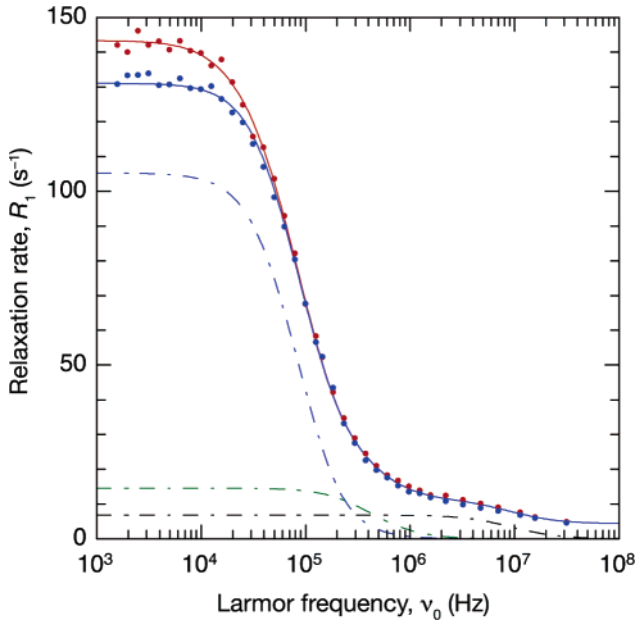

Figure 3. Water ^{2}H MRD profiles from agarose gels at 20.0 °C and pD 3.71 (red) or 7.36 (blue), both scaled to a concentration of 130 water molecules per monosaccharide unit. The dispersion curves resulted from a simultaneous fit to all data, where a hydroxyl contribution was allowed only at pD 3.71. The dashed curves represent the contributions from water components W1 (black), W2 (green), and W3 (blue). The hydroxyl contribution corresponds to the difference between the red and blue solid curves. The parameter values resulting from the fit are given in Table 1.

samples has been removed by normalization to the same number, $N_T = 130$, of water molecules per monosaccharide unit. The observed dispersion is caused by long-lived (>1 ns) water molecules trapped in the agarose structure and by exchanging hydroxyl deuterons.

The hydroxyl contribution to R_1 should be proportional to the exchange rate, $1/\tau_{OD}$ (see eq 7). The exchange is acid- and base-catalyzed according to

$$\frac{1}{\tau_{OD}} = k_1 10^{-pD} + k_2 10^{pD-pK_W} \qquad (9)$$

where pD = pH* + 0.41 and $pK_W = 15.13$ for D_2O at 20 °C.[40,41] Using hydrogen exchange rate constants determined for polysaccharides and simple carbohydrates,[42−45] we estimate that the exchange rate, $1/\tau_{OD}$, is 1−2 orders of magnitude higher at pD 3.71 than at pD 7.36. Because the ^{2}H dispersion profile varies little between these pD values (Figure 3), it must be strongly dominated by long-lived water molecules. Agarose contains only trace amounts of substituents (pyruvate[2]) that titrate in this pD range, so the gel structure should not depend on pD. The difference between the acidic and neutral dispersion profiles can therefore be attributed to hydroxyl deuterons. As expected from eq 7, this contribution is confined to low frequencies. (The minor differences between the two profiles at higher frequencies are deemed insignificant and may be due to small concentration or temperature errors.) Because the hydroxyl contribution is small even for the acidic sample, it should be negligibly small for the neutral sample. This prediction is confirmed by the following quantitative analysis.

Table 1. Results of a Simultaneous Fit to Water ^{2}H MRD Profiles at Two pD Values (Figure 3)

parameter (unit)	value
α (s^{-1})	4.38 ± 0.06
$N_{W1}S_{W1}^2$ (−)	0.121 ± 0.003
τ_{W1} (ns)	9.7 ± 0.2
$N_{W2}S_{W2}^2$ (−)	0.012 ± 0.001
τ_{W2} (μs)	0.21 ± 0.02
N_{W3} (−)	0.07 ± 0.01
S_{W3} (−)	0.64 ± 0.03
τ_{W3} (μs)	2.6 ± 0.8
x_{OD}/τ_{OD} (ms^{-1})	2.4 ± 0.1
S_{OD} (−)	0.24 ± 0.03

The two dispersion profiles (76 R_1 values) were fitted simultaneously with the model described in section 2.3. The fit is shown in Figure 3, and the resulting parameter values are collected in Table 1. The model includes three dispersive water components, denoted W1, W2, and W3 and described by seven parameters, in addition to the high-frequency parameter, α, which represents bulk and mobile surface water (see eq 8). The hydroxyl contribution is described by two parameters. In the following, we relate the values of these 10 parameters to the structure and dynamics of the agarose gel.

3.2. Dynamics of Hydroxyl Groups. Viewed along its axis, the agarose double helix has an approximately triangular cross-section (Figure 1c). If the agarose fibrils in the gel are built from six double helices,[3] then only 6 out of 18 faces are exposed. By symmetry, the hydroxyl groups must be evenly distributed among the three faces so the fraction solvent-accessible hydroxyl groups is $x_{OD} = {}^1/_3$. For thicker fibrils, with more than six double helices, x_{OD} will be smaller. If the inward-pointing GAL.HO2 (Figure 1b) exchanges much more slowly than the other three hydroxyls, we expect (for a fibril made up of six double helices) $x_{OD} = ({}^1/_3) \times ({}^3/_4) = {}^1/_4$. With $x_{OD} \leq {}^1/_3$, the value of x_{OD}/τ_{OD} deduced from the fit (Table 1) yields $\tau_{OD} \leq 0.14 \pm 0.01$ ms. This value refers to the acidic sample. Because the base-catalyzed process in eq 9 can be neglected at pD 3.71, we obtain a lower bound on the rate constant for acid-catalyzed exchange of hydroxyl deuterons: $k_1 \geq (3.7 \pm 0.2) \times 10^7\ M^{-1}\ s^{-1}$. This is similar to the value, $k_1 = 3 \times 10^7\ M^{-1}\ s^{-1}$, determined for glucose in H_2O at 23 °C from measurements of the transverse relaxation induced by exchange modulation of the ^{1}H chemical shift.[42] The primary kinetic H/D isotope effect is expected to be ~2 (values of 1.6 and ~3 have been reported for hydrogen exchange from water[46] and glucose[42]).

The small hydroxyl deuteron order parameter, $S_{OD} = 0.24 \pm 0.03$, can be rationalized in terms of fast internal motion. For a C−O−D angle of 109.5°, as expected for an sp^3 hybridized hydroxyl oxygen, free rotation of the O−D vector about the C−O bond reduces S_{OD} by the factor $[3\cos^2(180° - 109.5°) - 1]/2 = -{}^1/_3$. For this result to be applicable, rotation must be fast compared to hydrogen exchange (~0.1 ms) and the rotational barrier must be small (it is 1.0 kcal mol^{-1} for a free hydroxyl group according to the AMBER94 force field). This

(40) Covington, A. K.; Paabo, M.; Robinson, R. A.; Bates, R. G. *Anal. Chem.* **1968**, *40*, 700−706.
(41) Covington, A. K.; Robinson, R. A.; Bates, R. G. *J. Phys. Chem.* **1966**, *70*, 3820−3824.
(42) Hills, B. P. *Mol. Phys.* **1991**, *72*, 1099−1121.
(43) Hills, B. P.; Cano, C.; Belton, P. S. *Macromolecules* **1991**, *24*, 2944−2950.
(44) Poppe, L.; van Halbeek, H. *Nat. Struct. Biol.* **1994**, *1*, 215−216.
(45) Sandström, C.; Baumann, H.; Kenne, L. *J. Chem. Soc., Perkin Trans. 2* **1998**, 809−815.
(46) Halle, B.; Karlström, G. *J. Chem. Soc., Faraday Trans. 2* **1983**, *79*, 1031−1046.

is certainly the case at least for the three exposed hydroxyl groups (Figure 1b). We can then obtain the order parameter for the C−O bond as $S_{CO} = 3S_{OD} = 0.7 \pm 0.1$. (Because the relaxation rate involves the square of S_{OD}, we cannot determine the sign.)

Two important conclusions emerge from this analysis. First, the parameter values deduced from the fit are fully consistent with the known physicochemical properties of this and related systems. This agreement supports the generalized relaxation theory (notably, eq 7) on which our analysis of the acidic MRD profile is based. According to eqs 7 and 9, the hydroxyl contribution to the neutral MRD profile is obtained by scaling the hydroxyl contribution to the acidic profile by the factor $(k_2/k_1)10^{-4.06}$. With rate constants for glucose,[42] this contribution becomes 0.2 s^{-1} (or < 2% of the hydroxyl contribution to the acidic profile). Since this is an order of magnitude less than the experimental uncertainty in R_1 at the lowest frequencies, our neglect of the hydroxyl contribution at neutral pD is justified.

The second major conclusion is that the fraction solvent-accessible hydroxyl groups cannot be much less than $^1/_3$, since the hydrogen exchange rate constant k_1 required to account for the MRD data would then be too large. This imposes a restriction on the thickness of the agarose fibrils in the gel. If the cross-section of the agarose double helix is modeled as an equilateral triangle with a 15 Å side (Figure 1c), then the smallest symmetric fibril with six double helices has a diameter of 30 Å and an exposed hydroxyl fraction $x_{OD} = {}^1/_3$. A symmetric aggregate with a 90 Å diameter contains 54 double helices and has $x_{OD} = {}^1/_9$. If most agarose molecules were present in such aggregates, the MRD data would require an unrealistically large k_1 value, an order of magnitude larger than that for glucose.[42] Most of the agarose fibrils in the gel must therefore have a smaller diameter. This conclusion is consistent with small-angle X-ray scattering[3] and electron microscopy[4,5] studies, indicating a distribution of fibril diameters in the range 30−100 Å, with about half of the agarose molecules in 30 Å fibrils.[3]

3.3. Structure and Dynamics of Hydration Water. Information about the dynamics of the mobile (correlation times < 1 ns) water molecules interacting with the surface of the agarose fibrils can be derived from the parameter α, which corresponds to the high-frequency plateau of the dispersion profile.[31] With $R_{bulk} = 2.64$ s^{-1} and $N_T = 130$, we thus obtain $N_S(\langle\tau_S\rangle/\tau_{bulk} - 1) = 86 \pm 3$. Here, N_S is the number of water molecules per monosaccharide interacting with the agarose surface, and $\langle\tau_S\rangle$ is their average rotational correlation time. Previous ^{17}O magnetic relaxation studies of aqueous solutions of simple carbohydrates at 25 °C have reported values of 16−18 for this quantity (also on a monosaccharide basis) for glucose, galactose, and dextran.[47,48] For the vast majority of the water molecules interacting with the exposed agarose surface, the rotational retardation factor, $\langle\tau_S\rangle/\tau_{bulk}$, should be essentially the same as that for water molecules hydrating nonaggregated saccharides,[35] but N_S should be substantially smaller since much of the polysaccharide surface is buried in the agarose fibrils. Yet, $N_S(\langle\tau_S\rangle/\tau_{bulk} - 1)$ is a factor 5 larger than that for nonaggregated saccharides. This indicates that there is an additional (unobserved) dispersion step above 30 MHz due to a fourth class of water molecules with a correlation time less than, but possibly close to, ∼1 ns. These water molecules might be located in crevices between adjacent double helices in the fibril or at the connecting nodes in the gel network, where the fibril structure is disordered.

The slowest water component (W3), with residence time 2.6 μs and order parameter 0.64, is due to 0.07 water molecule per monosaccharide or 1 water molecule per 14 monosaccharide units. For the other two water components (W1 and W2), with residence times of 10 ns and 0.21 μs, we cannot separate the population from the order parameter. If all three components have the same order parameter ($S = 0.64$), their combined population becomes $N_{W1} + N_{W2} + N_{W3} = 0.30 + 0.03 + 0.07 = 0.40$ water molecules per monosaccharide. MRD studies of numerous globular proteins have shown that water residence times in the range 10^{-8}−10^{-5} s are invariably caused by entrapment in internal cavities.[49,50] We therefore attribute components W1, W2, and W3 to water molecules trapped within the agarose fibrils. Two types of internal hydration sites can be envisaged. On one hand, water molecules may occupy cavities at the interfaces of adjacent double helices, linking different agarose chains by H-bonds. For a fibril containing six three-fold double helices with 19 Å pitch[8] and 15 Å width, the MRD population of 0.4 water molecule per monosaccharide corresponds to 1 trapped water molecule per $19 \times 15/(3 \times 2 \times 2 \times 0.4) \approx 60$ Å^2 of interfacial area. Since the detailed structure of the fibril is not known, it is not possible to assess this alternative further.

On the other hand, it is possible that all the trapped water molecules responsible for dispersion components W1−W3 reside in the channel extending along the axis of each double helix in the fibril (Figure 1b). The structural model of the agarose double helix, although based on a small number of diffuse X-ray reflections, provides indirect support for a hydrated core.[8] These internal water molecules would stabilize the double helix by H-bonding to the GAL.O2 hydroxyl group and to the AGL.O5 pyranose ring oxygen of two agarobiose units from different strands.[8] Because each GAL.O2 and AGL.O5 atom is H-bonded to two water molecules, there is one internal water molecule per agarobiose unit, consistent with the UV absorption of dried agarose films.[51] This is also consistent with the MRD data, which yield a total population (components W1−W3) of 0.4 long-lived (10 ns−3 μs) water molecule per monosaccharide, not far from the value 0.5 expected from the crystal structure. If all three components are produced by equivalent, symmetry-related water molecules in the central cavity of the double helix, then they should have the same order parameter, as assumed in our estimate of the total population.

Although all internal water molecules are structurally equivalent in this model of the double helix, this does not imply that a single exchange rate (or residence time) should be observed for the gel. In fibrils with more than six double helices (section 3.2), water molecules are expected to exchange more slowly from the inner double helices than from the peripheral ones. Indeed, for sufficiently thick fibrils, water molecules in the innermost double helices may exchange too slowly to contribute to the measured ^2H relaxation rate. Furthermore, even for a thin

(47) Uedaira, H.; Ikura, M.; Uedaira, H. *Bull. Chem. Soc. Jpn.* **1989**, *62*, 1−4.
(48) Thomas, T. O.; Leyte, J. C. *Mol. Phys.* **1997**, *91*, 715−723.
(49) Denisov, V. P.; Halle, B. *Faraday Discuss.* **1996**, 103, 227−244.
(50) Halle, B. In *Hydration Processes in Biology*; Bellisent-Funel, M.-C., Ed.; IOS Press: Dordrecht, 1998; pp 233−249.
(51) Arndt, E. R.; Stevens, E. S. *Biopolymers* **1994**, *34*, 1527−1534.

fibril with six symmetry-related double helices, more than one correlation time may be observed. The survival probability probed by the MRD experiment is governed by the complex dynamics of the (aggregated) agarose double helix and may well exhibit a nonexponential decay. The three deduced correlation times for components W1−W3 may simply be the optimal multi-Lorentzian description of a more complex dispersion shape, reflecting a distribution of collective helix breathing modes. In conclusion, the MRD data are consistent with an internally hydrated agarose double helix, as proposed in connection with the fiber diffraction study.[8]

The structure shown in Figure 1 is based on the crystallographic coordinates of non-hydrogen atoms (PDB file 1AGA[8]), to which we added hydrogen atoms in standard geometry[52] and applied symmetry transformations to build a double helix containing 6 + 6 agarobiose units. We then added 10 water oxygens (O_W) at locations where they are equidistant from four potential H-bond partners, namely one GAL.O2 and one AGL.O5 from each strand. These O_W−O2 and O_W−O5 distances are all 2.71 Å, corresponding to strong H-bonds. The water oxygens are spaced 3.2 Å apart and lie close to the three-fold axis of the double helix. The six O−O_W−O angles are in the range 79°−136°, with an average of 109.7°, very close to the optimal tetrahedral angle. The water hydrogens were placed with standard water geometry (O−H bond length 0.976 Å and H−O−H angle 104°) and oriented so as to donate H-bonds symmetrically to one AGL.O5 atom from each strand. The O5−O_W−O5 angle is then 128°, so the deviation from a linear H-bond is only 12°. In the structure shown in Figure 1, the O−H bond of GAL.HO2 was rotated to minimize the distance to one of the two nearby water molecules. It is interesting to note that none of the substitutions found in agarose (sulfate, methoxy, pyruvate)[2] involves GAL.C2, suggesting that this hydroxyl group plays an important structural role.

While the H-bond geometry of the internal water molecules is nearly optimal, there is a van der Waals clash between the water oxygen and one of the nearby AGL.C5 carbon atoms, with an unphysically short O−C separation of 2.5 Å. However, the resolution of the X-ray fiber diffraction data[8] is only ∼3 Å, and the atom coordinates are averaged over variations in the covalent structure (such as the 6-sulfate form instead of the 3,6-anhydro form of the AGL unit). An early Monte Carlo study,[52] based on ab initio pair potentials, found that water molecules placed inside the cavity are not stably bound. Since the agarose double helix geometry was fixed in the simulation, this finding may simply be a consequence of the van der Waals clash with AGL.C5. Also in a short MD simulation with an early version of the AMBER force-field (with an explicit H-bond term), the central cavity of the double helix was not found to favor water occupation.[53] However, the force field used in this study may not be sufficiently accurate and/or the agarose double helix geometry may not have been fully equilibrated. Further simulation and modeling studies may clarify this issue.

3.4. Temperature Dependence. For the slowest water component (W3), the residence time, $\tau_{W3} = 2.6\ \mu$s, exceeds the inverse residual quadrupole frequency, $1/\Omega_{Q,W3} = 1.5\ \mu$s. Since the exchange of these water molecules must be faster at higher temperatures, eqs 3−5 predict that the contribution of water component W3 to R_1 at low frequencies should first increase with temperature and then pass through a maximum. This prediction is confirmed by the results in Figure 4, showing the temperature dependence of R_1 at 1.5 kHz for an agarose CPG/LE gel at pD 7.51, where the hydroxyl contribution is negligible. Since the melting temperature of this agarose preparation is 87 °C (at 1.5% agarose), we can expect some structural changes at the highest investigated temperatures. To check for such changes, we exploited the pronounced setting−melting hysteresis of agarose gels.[11,16] The data in Figure 4 were obtained from a heating sequence, where 30 min of thermal equilibration was allowed after each 5 °C temperature increase. In separate control experiments, after every temperature increment, we cooled the sample by 10 or 15 °C and remeasured R_1 at the lower temperature. Because of the hysteresis, the gel then retains the same structure as that at the higher temperature as long as we remain above the gel setting temperature (∼35 °C). We thus inferred significant structural changes at 65 and 70 °C, and a correction was applied to compensate for this (Figure 4).

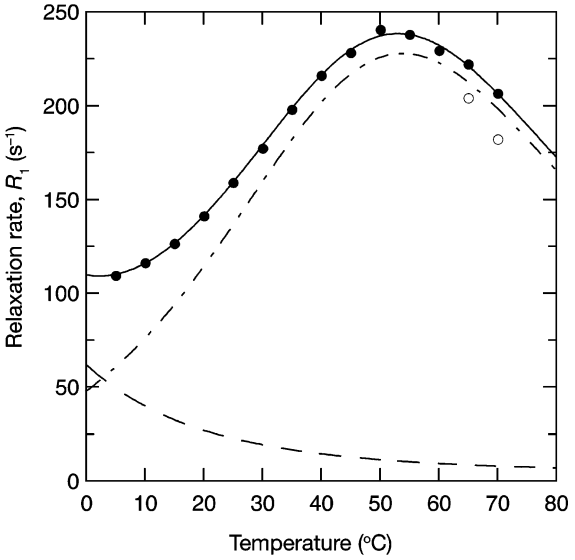

Figure 4. Temperature dependence of the water ^{2}H relaxation rate at 1.5 kHz for an agarose gel with $N_T = 124.6$ and pD 7.51. The R_1 values measured at the two highest temperatures (open symbols) have been corrected for temperature-induced changes in gel structure. The solid curve resulted from a four-parameter fit, with the parameter values in Table 2. The other curves represent the contribution to R_1 from water components W1 + W2 (dashed) and W3 (dash−dotted).

The temperature dependence of R_1 was analyzed with the relaxation theory described in section 2.3. On the low-frequency plateau of the dispersion profile, where we can set $\omega_0 = 0$, we have

$$R_1(0) = \alpha + \frac{2}{3N_T}(N_{W1}\Omega_{Q,W1}^2\tau_{W1} + N_{W2}\Omega_{Q,W2}^2\tau_{W2}) + \frac{2}{3N_T}\frac{N_{W3}\Omega_{Q,W3}^2\tau_{W3}}{1 + (\Omega_{Q,W3}\tau_{W3})^2} \quad (10)$$

We assume that N_{Wk} and S_{Wk} are independent of temperature and neglect the temperature dependence in the small α contribution (Table 1). The Arrhenius law is used to model the temperature dependence of the residence times, $\tau_{Wk} \approx \exp(E_A/$

(52) Corongiu, G.; Fornili, S. L.; Clementi, E. *Int. J. Quantum Chem., Quantum Biol. Symp.* **1983**, *10*, 277−291.
(53) Haggett, N. M. W.; Hoffmann, R. A.; Howlin, B. J.; Webb, G. A. *J. Mol. Model.* **1997**, *3*, 301−310.

Table 2. Results of Fit to Water-^{2}H R_1 at 1.5 kHz and 5−70 °C (Figure 4)

parameter (unit)	value
$\tau_{W3}(20\ °C)/N_{W3}$ (μs)	43.7 ± 0.6
$S_{W3}\tau_{W3}(20\ °C)$ (μs)	3.5 ± 0.1
$A_{1,2}$ (ns)	3.7 ± 0.1
E_A (kJ mol^{-1})	30.9 ± 0.5

RT), with the same activation energy, E_A, for the three water components. The fit in Figure 4 involves four independent parameters, which may be chosen as $\tau_{W3}(20\ °C)/N_{W3}$, $S_{W3}\tau_{W3}(20\ °C)$, $A_{1,2} = N_{W1}S_{W1}^2\tau_{W1}(20\ °C) + N_{W2}S_{W2}^2\tau_{W2}(20\ °C)$, and E_A. The resulting values for the first three of these parameters (Table 2) are consistent with the parameter values deduced from the MRD profiles in Figure 3. From Table 1, we thus obtain $\tau_{W3}(20\ °C)/N_{W3} = 37 \pm 13$ μs and $A_{1,2} = 3.7 \pm 0.8$ ns, not significantly different from the values in Table 2, and $S_{W3}\tau_{W3}(20\ °C) = 1.7 \pm 0.5$ μs, which differs by a factor 2 from the value deduced from the temperature dependence. The activation energy, $E_A = 30.9 \pm 0.5$ kJ mol^{-1}, is surprisingly small for the exchange of deeply buried water molecules.[50,54] E_A is essentially determined by the slowest W3 component, which accounts for 95% of R_1 at the maximum (Figure 4). Both the relatively small E_A and the factor-2 discrepancy in $S_{W3}\tau_{W3}(20\ °C)$ might be explained by an exchange mechanism involving a distribution of collective breathing modes in the agarose double helix, where the mode amplitudes as well as the mode relaxation times depend on temperature. The temperature dependence would then be more complex than that predicted by the Arrhenius law.

3.5. Comparison with Previous NMR Relaxation Studies. The present work goes beyond previous ^{2}H NMR relaxation studies[11,16,18] of agarose gels in three important respects. First, whereas previous studies have been confined to one or a few high frequencies (4−25 MHz), we have measured the ^{2}H dispersion over a wide frequency range (1.5 kHz−30 MHz). This allows a more complete and accurate dynamic characterization of the system. Second, we are not aware of any previous NMR relaxation studies of agarose gels at variable pH, even though pH variation is the most direct way of distinguishing water and hydroxyl contributions. In fact, in most previous studies the pH of the gel was not even reported. Third, the conventional BWR theory has been used in all earlier work, although this theory breaks down for ^{2}H correlation times on the order of 1 μs or longer. We describe the contributions from slowly exchanging water molecules (component W3) and hydroxyl deuterons with an SLE-based theory,[23] which remains valid over the full range of correlation times and nuclear coupling frequencies.

From ^{2}H relaxation data recorded at ∼10 MHz on an agar gel with $N_T = 108$ at 25 °C, Woessner and Snowden deduced a correlation time of 6 ns and (in our notation) $NS^2 = 0.2$.[18] These values are similar to our results for water component W1 (Table 1), which dominates the frequency dependence in the megahertz range (Figure 3). However, Woessner and Snowden attributed the megahertz R_1 relaxation enhancement to hydroxyl deuterons. Although the underlying molecular motion was not discussed, the only plausible candidate is the O−D bond rotation that is also manifested in the order parameter S_{OD} in the residual quadrupole coupling that is averaged to zero by the much slower hydroxyl deuteron exchange (section 3.2). Using the parameter values deduced from our data, it can be shown that this internal-motion contribution to R_1 is not in the fast-exchange regime even at pD 3.71 and that it should be 1−2 orders of magnitude smaller at pD 7.36. Since the observed pD dependence in the megahertz frequency range is hardly significant (Figure 3), we conclude that the 10 ns dispersion component (W1) is due to water molecules rather than to hydroxyl deuterons.

Woessner et al. also measured the transverse relaxation rate, R_2, which reports on slow motions even if measured at high frequencies.[16,18] The observation that $R_2 \gg R_1$ at megahertz frequencies is consistent with the large R_1 dispersion seen here below 1 MHz. Woessner et al. attributed the large R_2 to a small fraction of "strongly bound water" with a correlation time of 0.5 μs at 25 °C. This value is a factor of 5 smaller than what we find for component W3 (Table 1), primarily because Woessner et al. used the conventional BWR theory and described their R_1 and R_2 data in terms of two (rather than three) correlation times. Furthermore, they interpreted the microsecond correlation time in terms of slow localized rotation of bound water (at unspecified locations), rather than as an exchange time (or mean residence time) of irrotationally bound internal water molecules.

Several studies of agarose gels have shown that R_2 exhibits a maximum as a function of temperature.[17−19,20,24] In particular, Woessner and Snowden found a broad maximum of $R_2(^2H)$ at 42 °C in an ∼7% agar gel.[18] Because $R_1 = R_2$ at zero frequency, these earlier observations are consistent with our finding of a temperature maximum in R_1 on the low-frequency plateau of the dispersion profile. The R_1 maximum observed here occurs at somewhat higher temperature (53 °C), but this minor difference may be attributed to differences in the agarose preparations and to stronger premelting effects in previous studies.

Finally, we note that water ^{17}O R_1 and R_2 measurements at 8 MHz have been reported for a 5% agarose gel.[55] The observed ratio $R_2/R_1 = 2.6$ (at 20 °C) indicates water motions on the time scale of 10^{-8} s or slower, consistent with our findings. An analysis using the SLE expressions appropriate for the spin-$^5/_2$ ^{17}O nuclide (T. Nilsson and B. Halle, to be published) indicates that the ^{17}O R_1 value is consistent with our ^{2}H MRD results (and a reasonable H/D isotope effect for the correlation times). The measured ^{17}O R_2 value is larger than that predicted on the basis of our ^{2}H results, but it may include a contribution from modulation of the ^{17}O−^{1}H scalar spin coupling by proton exchange in bulk water.[46]

4. Concluding Remarks

Agarose gels have been known for half a century to produce an exceptionally large enhancement of the water ^{1}H and ^{2}H magnetic relaxation rates.[9] The molecular basis of this effect has not been uncovered despite the importance of agarose gels as chromatographic and electrophoretic media,[56] as stabilizers and thickeners in food preparations and pharmaceutical products,[1] and as models for biological tissues in connection with clinical MRI studies.[23−25] By measuring the ^{2}H relaxation

(54) Denisov, V. P.; Peters, J.; Hörlein, H. D.; Halle, B. *Nat. Struct. Biol.* **1996**, *3*, 505−509.
(55) Ablett, S.; Lillford, P. J. *Chem. Phys. Lett.* **1977**, *50*, 97−100.
(56) Fatin-Rouge, N.; Milon, A.; Buffle, J.; Goulet, R. R.; Tessier, A. *J. Phys. Chem. B* **2003**, *107*, 1216−12137.

dispersion profiles over an extensive frequency range (>4 decades), we have avoided the interpretational ambiguity associated with more limited data sets. Moreover, by using a more general theory of nuclear spin relaxation in systems of immobilized macromolecules,[23] we have identified the molecular species and motions responsible for the unusual magnetic relaxation behavior of agarose gels. In particular, we have demonstrated that the relaxation dispersion from neutral agarose gels is produced by the exchange of a small number of water molecules temporarily trapped within the agarose fibrils. We have also shown that this interpretation is quantitatively consistent with the temperature maximum in R_1 on the low-frequency plateau.

Our results suggest that these internal water molecules are located in the central cavity of the agarose double helix, as originally proposed on the basis of fiber diffraction data.[8] We propose that these water molecules exchange with bulk water by helix breathing modes on time scales ranging from 10^{-8} to 10^{-6} s. In acidic gels, we have also identified a modest contribution at low frequencies from exchange of solvent-accessible hydroxyl deuterons on a time scale of 10^{-4} s. The observed relaxation dispersion can be fully accounted for by the exchange of trapped water molecules and, at low pH, of hydroxyl deuterons, with no need to invoke any other motions.

The water ^{2}H relaxation dispersion from aqueous solutions of freely tumbling proteins is also produced by trapped internal water molecules and labile macromolecular deuterons.[31,49,50] In that case, however, the molecular motion that determines the frequency dependence of the magnetic relaxation rate is the rotational diffusion of the protein molecules. Therefore, it is usually only possible to obtain lower and upper bounds for the rate of exchange of internal water molecules. In gels and other systems with rotationally immobilized macromolecules, internal water exchange can be studied more directly because it is then the exchange process itself that produces the frequency dependence of the relaxation rate. If the exchange is sufficiently fast, the conventional motional-narrowing approximation is valid and the dispersion frequency equals the exchange rate. However, for agarose gels and most other aqueous systems with rotationally immobilized macromolecules, the relaxation dispersion is dominated by slow exchange processes and cannot be described by the conventional relaxation theory. The more general, SLE-based relaxation theory used here is valid over the full range of exchange rates and nuclear (quadrupole and Zeeman) evolution frequencies and provides a quantitatively accurate description of the observed relaxation dispersion. As discussed elsewhere,[27,28] these insights are crucial for understanding the molecular basis of water ^{1}H relaxation in biological tissues and of intrinsic image contrast in clinical MRI.

Acknowledgment. This work was supported by the Swedish Research Council and the Knut and Alice Wallenberg Foundation.

JA058837N